

**Abstract**

Dark matter is hypothetical matter which does not interact with electromagnetic radiation. The existence of dark matter is only inferred from gravitational effects of astrophysical observations to explain the missing mass component of the Universe. Weakly Interacting Massive Particles are currently the most popular candidate to explain the missing mass component. I review the current status of experimental searches of dark matter through direct detection using terrestrial detectors.

**1. Introduction**

One of the biggest puzzles in astroparticle physics is that 95% of the energy component of the Universe cannot be explained by ordinary matter. There is an increasing consensus that 72% of the Universe consists of an unknown energy component and 23% of the Universe consists of an unknown matter component. The observations of rotational curves of galaxies, large scale structures, galaxy clusters, colliding clusters, gravitational lensing, and Cosmic Microwave Background (CMB) observations provide strong evidence that a nonluminous, nonbaryonic component, so called dark matter, may constitute most of the matter in the Universe [1, 2]. However all these observations are based on gravitational interactions. We do not have clear answers yet even for simple questions such as, "Do they interact with normal matter other than through gravitation forces?", "Are they a type of particle?", "How heavy they are?", "Do they have spin?", "Do they consist of single types of particles or compositions of many particles?", "Is their distribution clumpy or uniform in our local Universe?" All unknown! This unconstrained condition allows a lot of room for speculation of the possible candidates of dark matter.

There are increasing astrophysical observations that indicate excess of signals above the expected astrophysical processes or background level. Most recently, PAMELA [3], ATIC [4], Fermi/LAT [5] and HESS [6] Collaborations observed an excess of positron and electron signals at around 100 GeV  $\sim$  TeV of energy. The excess of positrons (and electrons) is readily interpreted as an enhancement of dark matter through co-annihilations into the leptonic channel. These interpretations, however, usually requires unrealistically higher dark matter density profile. Interestingly and historically, any kind of excess of this observational nature above the known background sources rarely failed to be interpreted as an enhancement of dark matter even before a full investigation of possible background sources and systematic issues of detection had been completely resolved. A fashion like this is mainly due to the unconstrained dark matter conditions and simply reflect the fact that we do not know very well about the characteristics of the dark matter. Therefore, answering the question whether dark matter is interacting with normal matter or not is one of the keys to resolve various unexplained astrophysical observations. For more details regarding these interesting adventures on astrophysical observations and their interpretations, the reader may refer to the review of indirect detection of dark matter in these conference proceedings. In this review, I will focus on the direct

detection experiments of dark matter.

**2. Direct Detection of Dark Matter**

Given the fact that the only evidence of the dark matter is from gravitational observations, it maybe a reasonable to apply Modified Newtonian Dynamics (MOND) in the galactic scale, a nostalgia of general relativity [7]. The MOND theory does indeed successfully explain the galactic rotational velocity curves where the rotational velocity of stars becomes constant as it goes further and further away from the galactic center. However, the MOND theory is confronted with difficulties when trying to explain recent observations such as Bullet Clusters [8], and no successful cosmology can be built based on the theory yet.

The dark matter hypothesis is currently the most popular solution to address the majority of astrophysical and cosmological observations. There is no lack of particle dark matter candidates. However, weakly interacting massive particles (WIMPs) [9] are currently the most interesting for two reasons. First, WIMPs are naturally present in supersymmetric and extra-dimensional scenarios, and it is relatively simple to construct a stable particle in a cosmological time scale by requiring certain symmetries (such as R-parity in supersymmetric model or KK-parity in universal extra-dimension model). Second, the expected interaction cross-section of WIMPs with normal matter and its mass range are the most experimentally accessible among any other dark matter candidates [10, 11, 12].

For a direct detection experiment using terrestrial detectors, one has to make a big assumption that dark matter is interacting with normal matter and they leave a detectable signal in the target material. Density profiles and velocity distributions of a dark matter halo and dark matter interaction cross-section are the key elements to precisely estimate interaction rates of dark matter in a direct detection experiment. A standard prescription that most of the direct detection experiments follow in order to report their results is from reference [13]. The distribution of dark matter is usually assumed to form a roughly isothermal spherical halo around our Galaxy with a Maxwell-Boltzmann velocity distribution at a mean of  $\sim 230$  km/sec, and an escape velocity from the Galactic halo of  $\sim 650$  km/sec. The local dark matter halo density which is inferred from the rotational curves of galaxy is about  $0.3 \text{ GeV/cm}^3$ .

At the zero-momentum transfer limit, the elastic scattering cross-section of WIMPs on nuclei can be written as  $\sigma_{\chi A} = 4G_F^2 \mu^2 C_A$ , where  $G_F$  is the Fermi constant. The  $\mu$  is the reduced mass of a dark matter particle ( $\chi$ ) and recoil nucleus ( $A$ ). In case of spin-independent (scalar) interactions,  $C_A = 1/4\pi[Zf_p + (A - Z)f_n]^2$ . Assuming equal strengths of the proton ( $f_p$ ) and neutron ( $f_n$ ) coupling, the cross-section is proportional to the atomic mass squared ( $A^2$ ). Atomic form factors should be considered for a realistic finite momentum transfer. The expected event rate depends on the experimental energy thresholds. For example, Fig 1. shows expected event rates of dark matter at some given spin independent cross-section for xenon, germanium and argon targets. At zero momentum transfer, the best event

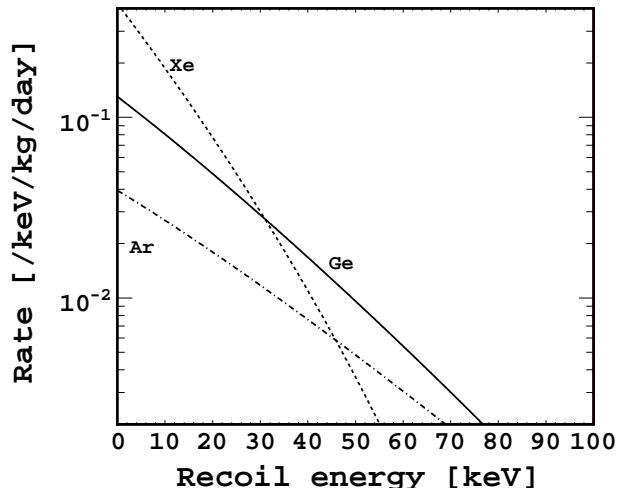


Fig. 1. Differential interaction rates for germanium (solid-line), xenon (dotted-line), and argon (dash-dot) for some arbitrary spin-dependent (scalar) coupling scale.

rate can be obtained in a xenon ( $A=131.29$ ) target for a given mass compared to germanium ( $A=72.61$ ) and argon ( $A=39.95$ ). However, due to the atomic form factor correction, the total event rate depends on the detector energy thresholds; in general, lower the energy threshold provides the better dark matter detection sensitivity given the same background configuration. In case of the spin-dependent (axial) interactions,  $C_A = 8/\pi[a_p\langle S_p\rangle + a_n\langle S_n\rangle]^2(J+1)/J$ , where  $\langle S_p\rangle$  and  $\langle S_n\rangle$  are the nuclear spins.  $a_p$  and  $a_n$  are the coupling strengths. Therefore having enriched spin-odd materials are beneficial to enhance the spin-dependent interactions.

The mass range below 500 GeV is particularly interesting. In this range, together with the velocity distributions discussed above, the WIMP-nucleon scattering would result in an energy deposition in the detector of a few to tens of keV. Most of the direct detection experiments are designed to detect nuclear recoil by elastic scattering of WIMPs.

A real challenge of direct searches of dark matter is the extremely low background requirement of these experiments. In order to detect a non-Standard Model particle, all Standard Model particles that can be seen by the detector must be treated as background sources. Once all background sources are identified or removed, the remaining events that cannot be understood within the Standard Model scheme are candidates for new particles. Therefore the major efforts of any dark matter search experiment are in fact mostly about reduction of backgrounds. Dark matter searches are probing a domain of ultra-low radioactive backgrounds which have never been probed before. The number of event counts in this extreme region of cross-section is one event in an order of  $10^3$  kg-days of detector exposure (keV of energy ranges and  $\sigma < 10^{-44}\text{cm}^2$ ). Accordingly, in order to achieve the next generation (G2) goal of sensitivity ( $\sigma < 10^{-47}\text{cm}^2$ ), the background level should be controlled at the level of one event count in  $10^6$  kg-days of detector exposure – a daunting task. Direct search detectors must be built with materials of extremely low radioactivity, and protected from the ambient backgrounds by efficient shields.

Cosmic-ray activation should be reduced by constructing the detectors in deep-underground sites.

Given the uncertainties associated with the ultra-low background required for these experiments, it is important to develop detectors with more than one type of target nucleus in order to probe the  $A^2$ -dependence of the cross-section.

### 3. Experiments

The two leading classes of experimental design are based either on solid-state detectors or liquefied noble gases. The Cryogenic Dark Matter Search (CDMS) experiment uses germanium and silicon crystals as the detector target materials that read out phonon and ionization signals using superconducting sensors in a cryogenic environment [14]. The CDMS detector is the only proven technology that has demonstrated zero background in the WIMP search signal region although the fabrication technique of a large scale crystal detector has yet to be demonstrated. On the other hand, XENON and LUX (Large Underground Xenon) experiments use liquid-gas dual-phase Xenon Time Projection Chambers (XeTPC) to readout both scintillation and ionization signals and whose technical feasibility has been recently demonstrated by the XENON-10 collaboration although the rejection power of the backgrounds needs to be demonstrated [15]. Each technique has its own advantages and drawbacks. Another type of liquid noble gas technique which may potentially achieve world leading sensitivity of dark matter within a few years is a single phase (liquid) noble gas detector technique. This type of detector does not have substantial discrimination power between nuclear and electron recoil interactions and hence it is necessary to keep all background sources away from the detector's fiducial volume. A leading experiment that is close to the operation of this type of detector is the XMASS experiment [16].

Currently, the best experimental upper bound for spin-independent coupling is set by the CDMS experiment ( $\sigma < 4.6 \times 10^{-44}\text{cm}^2$  for WIMPs masses above  $42\text{ GeV}/c^2$ ) [14]. The XENON [15] experiment set the best limit at lower masses. The best spin-dependent interaction limit on protons is set by COUPP [17] and KIMS [18] ( $\sigma_{SD-p} < \sim 10^{-37}\text{cm}^2$ ), while the best spin-dependent interaction limit on neutrons is set by the XENON-10 experiment ( $\sigma_{SD-n} < \sim 10^{-39}\text{cm}^2$ ) [19].

#### 3.1. CDMS

The CDMS experiment is designed to detect a WIMP signal through nuclear recoil by elastic scattering. The detector is capable of reading out both the phonon energy and the ionization energy of an interaction in germanium or silicon crystals. The idea of the CDMS detector is to discriminate WIMP-nuclear recoil energy by measuring both the ionization and phonon signal from the crystal. The detector is an ultra-pure germanium ( $\sim 250\text{ g}$ ) or silicon ( $\sim 100\text{ g}$ ) crystal in a cylindrical shape of 1 cm thickness and 7.6 cm in diameter. A tower consists of a vertically stacked 6 crystal detector array. The detectors are cooled by a dilution refrigerator down to 50 mK. This cryogenic configuration prevents background signals caused by atomic thermal excitations in the crystal. The ionization signal is the interaction that breaks the electron-hole pairs of the semiconductor crystal. The electron and hole pairs are separated by an electric field through the crystal. The ionization signals are then read out by inner and outer electrodes. The inner electrode covers 85% of the ionization side of the detector. The events from the edge

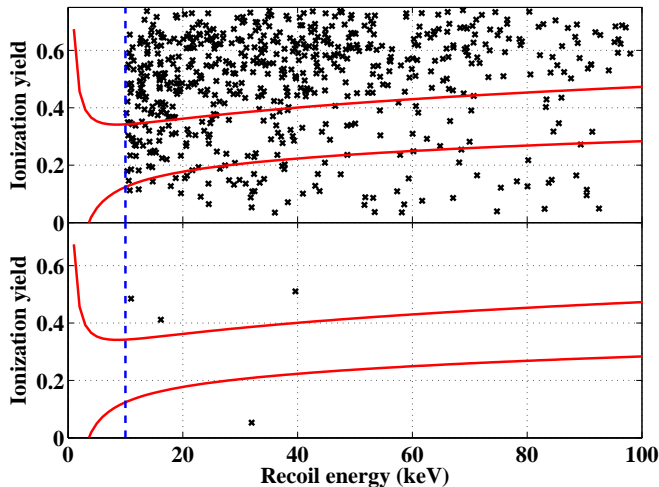


Fig. 2. Result from CDMS experiment. (top) Ionization yield versus recoil energy in all CDMS detectors passing all cuts before electron rejection cut. (bottom) the same but after electron rejection. No event was found within the nuclear recoil band, a WIMP search signal region. Figure is taken from [14].

area of the detector have suppressed phonon energy collections and the outer electrode is used to discriminate those edge-events. The phonon signals that are produced by the vibration of crystal lattices are read out by a total of 4144 Quasiparticle-assisted Electrothermal-feedback Transition-edge sensors (QETs) on each detector. Each QET consists of a  $1\ \mu\text{m}$  wide strip of tungsten connected to 8 superconducting aluminum collection fins which cover the phonon sensor side of the crystal. The tungsten strips, on Transition-Edge-Sensors (TESs), are voltage biased, with the current through them monitored by a high-bandwidth SQUID array.

When an interaction occurs in the crystal, a huge amount of phonons are produced. Most of the phonons that reach the surface of a phonon sensor area can scatter into the aluminum fins. The athermal phonons, energetic enough (above  $340\ \mu\text{eV}$ ) to break Cooper pairs in a superconducting state of aluminum fins, produce quasiparticles. The quasiparticles enter into the TESs. The interaction between the quasiparticles and conduction electrons in the TESs increases the temperature of the system and hence increases the resistance of the tungsten. The increase of resistance decreases the current supplied by the voltage bias. The reduction of Joule heating from the voltage bias lowers the temperature of the tungsten. This strong electro-thermal-feedback guarantees that the power deposited into the TES is exactly compensated for by a reduction in Joule heating. Then the energy deposited is measured by reading out the change of current.

The ionization yield is determined by the ratio of ionization energy to the recoil energy, which gives a discrimination of electron recoil events (yield  $\sim 1$ ) and nuclear recoil events (yield  $\sim 0.3$ , where WIMP signal expected). Some surface electron events leak into the lower yield area where nuclear recoil events are expected due to insufficient charge collection. However, those electron events show faster phonon signals and therefore can be selected out from the nuclear recoil events. The effective exposure before the cuts is 397.8 kg-days, and the net exposure after applying all the background rejection cuts is 121.3 kg-days (averaged over recoil energies 10–

100 keV, weighted for a WIMP mass of  $60\ \text{GeV}/c^2$ ). No events were observed in the WIMP search signal region while the total expected background in the signal region was less than 0.6 event (see Fig. 2.). The upper panel shows the ionization yield distribution versus energy for single-scatter events passing all selection cuts except the timing cut. The four events passing the timing cut shown in the lower panel are outside the  $2\sigma$  nuclear recoil region. The results are consistent with null observation of WIMPs (none of the non-Standard Model particles were observed within the detector sensitivity).

The CDMS collaboration has accumulated more than 1-ton days of WIMP search data. The results of the data analysis is expected at the end of 2009. SuperCDMS detectors, a 1 inch thick ( $\sim 650\ \text{g}/\text{detector}$ ) with a new detector sensor design, have been installed at Soudan in the middle of 2009 and currently running with stable condition. The SuperCDMS collaboration is preparing for the next generation of arrays with total germanium masses of 100 kg phase and eventually ton scale experiments.

### 3.2. XENON

The XENON-10 collaboration operated a 15 kg dual-phase (liquid and gas) xenon time projection chamber (XeTPC) in the Gran Sasso Underground Laboratory. The XENON-10 experiment uses two arrays of UV-sensitive photomultipliers (PMTs) to detect the prompt scintillation light (175 nm) and proportional light signals induced by particles interacting in the sensitive liquid xenon (LXe) volume. The excellent 3 dimensional position sensitivity, the self-shielding of backgrounds, and the prompt versus proportional light ratio are the features of the background rejection. The first results with  $\sim 136$  kg-days of net exposure demonstrated that LXe can be used for stable, homogeneous, large scale dark matter detectors which provide excellent position resolution and discrimination against the electron recoil background.

XENON-10 collaboration collected WIMP search data between August 2006 and February 2007. The first XENON-10 results leave 10 background events in its dark matter signal region (see Fig 3.). The upper bound of spin-independent cross-sections on nucleons is  $4.5 \times 10^{-44}\ \text{cm}^2$  for a WIMP mass of  $30\ \text{GeV}/c^2$ . The natural xenon contains  $^{129}\text{Xe}$  (26.4%) and  $^{131}\text{Xe}$  (21.2%) isotopes, each of these having an unpaired neutron. Therefore the XENON-10 results substantially constrain the spin-dependent WIMP-nucleon cross-section.

The next phase, XENON-100, will operate a total of 170 kg (70 kg fiducial) of xenon, viewed by 242 PMTs, in a dual-phase TPC in an improved XENON-10 shield at the Gran Sasso Laboratory. While the fiducial mass is increased by an order of magnitude, the background will be lower by about a factor of 100 (through careful selection of ultra-low background materials, the placing of cryogenic devices and high-voltage feed-throughs outside of the shield and by using 100 kg of active LXe shield) compared to XENON-10. With all these efforts, XENON-100 is aiming to demonstrate a background free configuration and the WIMP search sensitivity down to  $\sim 2 \times 10^{-45}\ \text{cm}^2$ .

### 3.3. KIMS

The Korea Invisible Mass Search (KIMS) experiment [18] is located at the Yangyang Underground Laboratory, Korea. The collaboration has operated four low-background CsI(Tl) crystals, each viewed by two photo-

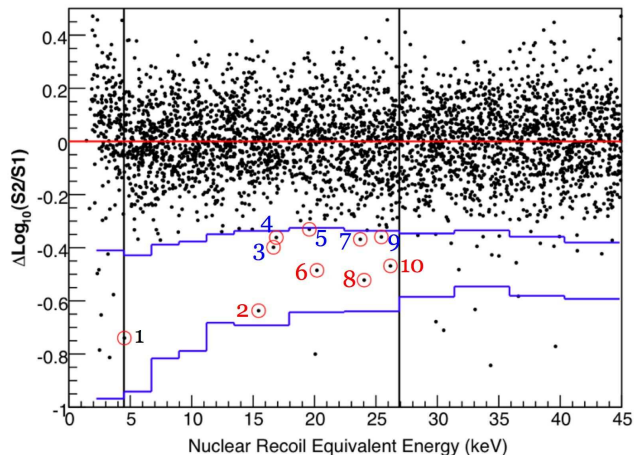


Fig. 3. Results from XENON-10 experiment. The WIMP search energy window was defined between two vertical lines. Figure is taken from [15].

multipliers, for a total exposure of 3409kg-days. Both  $^{133}\text{Cs}$  and  $^{127}\text{I}$  are sensitive to the spin-dependent interaction of WIMPs with nuclei. KIMS detects the scintillation light after a particle interacts in one of the crystals. The pulse shape discrimination technique, using the time distribution of the signal, allows to statistically separate nuclear recoils from the electron recoil background. The KIMS results are consistent with a null observation of a WIMP signal yielding the best limits on spin-dependent WIMP-proton couplings for a WIMP mass above  $30\text{ GeV}/c^2$ . The upper bound for a WIMP mass of  $80\text{ GeV}/c^2$  is  $1.7 \times 10^{-37}\text{ cm}^2$ .

### 3.4. COUPP

The Chicagoland Observatory for Underground Particle Physics (COUPP) experiment [17] is operated at Fermilab, USA. The experiment has revived the bubble chamber technique for direct WIMP searches. The superheated liquid can be tuned such that the detector responds only to keV nuclear recoils, being fully insensitive to minimum ionizing particles. A 1.5 kg chamber of superheated  $\text{CF}_3\text{I}$  has been operated for a total exposure of 250 kg-days. The presence of fluorine and iodine in the target makes COUPP sensitive to both spin-dependent and spin-independent WIMP-nuclei couplings. The production of bubbles is monitored optically and via sound emission, reaching a reconstructed 3 dimensional spatial resolution of  $\sim 1\text{ mm}$ . It allows to reject boundary-events and to identify multiple neutron interactions. The COUPP results set the most sensitive limit on spin-dependent WIMP-proton cross-sections for a WIMP mass below  $30\text{ GeV}/c^2$  ( $\sigma > 2.7 \times 10^{-37}\text{ cm}^2$  at a WIMP mass of  $40\text{ GeV}/c^2$ ). A 60 kg phase COUPP chamber is under construction at Fermilab for operational test and plan to move to SNOLAB.

### 3.5. Comments on DAMA results

DAMA is the only experiment who claims evidence of the direct detection of dark matter. The data from DAMA/NaI [20] and subsequent results from DAMA/LIBRA [21] with a total exposure of 0.82 ton-yr show a clear modulation signal with  $8.2\sigma$  significance.

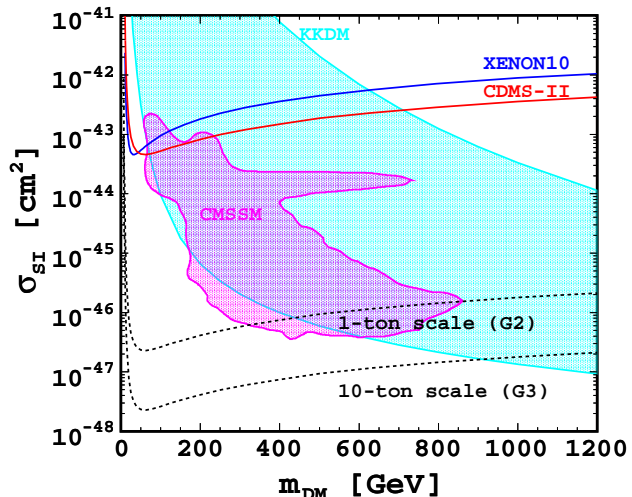


Fig. 4. Spin-independent WIMP-nucleon cross-section upper limits (90% C.L.) versus WIMP mass. CDMS-II and XENON-10 are the current best upper bounds. The predicted cross-section and mass area for Kaluza-Klein Dark Matter [11] and constrained minimal supersymmetry (CMSSM) model [34] is the shaded regions. Future ton-scale and multi-ton scale detector sensitivities (dotted-line) will cover most of the model parameter spaces.

The phase of this modulation is consistent with that expected from the dark matter halo of our Galaxy due to the movement of the earth around the sun. Therefore, it is fair enough to state that the DAMA annual modulation signature itself can be regarded as a very strong possible evidence of dark matter. The real problem arises that no other experiment has yet to confirm the claimed DAMA observation.

The standard interpretation of spin-independent elastic WIMP-nucleon scattering accounting for the DAMA modulation is tightly constrained by bounds from several experiments, most clearly from CDMS and XENON-10 although light WIMPs with  $< 10\text{ GeV}$  masses might be marginally compatible with the constraints [22, 23, 24, 25, 26]. Spin-dependent couplings to protons constrained by COUPP, KIMS and PICASSO [27].

Inelastic scattering of a dark matter particle to a nearly degenerate excited state has been proposed in [28, 29] for recent analyses, though also in this case tight constraints apply, in particular from CRESST-II [30], ZEPLIN-II [31], and XENON-10 [32]. The other possible interpretation of DAMA result which is not completely ruled out by other experiments yet is electron-recoil dark matter concept [33].

## 4. Prospects and conclusions

Based on very strong astrophysical evidence of the existence of dark matter, a huge effort has been made for direct search experiments. As it is shown in Fig 4., future multi-ton scale experiment(s) will eventually be able to probe most of the well motivated model parameter regions. Technical development has been substantially improved during the last decades for both detector fabrication and reduction of radioactive backgrounds. Currently, the CDMS experiment is leading the sensitivities of direct searches and is the only proven technology which demonstrates background-free detector construction and operation. The XENON and LUX col-

laborations will soon answer the questions whether the dual-phase LXeTPC technology is adequate to a future multi-ton scale dark matter search detector. XMASS in Japan will operate in a few months and will address whether the simpler single phase xenon detector is indeed a better concept for the direct search. Although there is very steep competition among the various collaborations, these efforts will eventually answer the long standing profound question: What Universe made of?

## References

- [1] D. N. Spergel et al., (WMAP Collab.), *Astrophysics Journal* 148, 175, 2003; M. Tegmark et al., (SDSS Collab.), *Phys. Rev. D* 69, (2004) 103501.
- [2] E. Komatsu, et al., *Astrophys. J. Suppl.* 180 (2009) 330.
- [3] O. Adriani et al. [PAMELA Collaboration], *Nature* 458 (2009) 607 .
- [4] J. Chang et al. [ATIC Collaboration], *Nature* 456, (2009) 362.
- [5] A. A. Abdo et al. *Phys. Rev. Lett.* 102, (2009) 181101.
- [6] F. Aharonian et al, arXiv:0905.0105.
- [7] M. Milgrom, *Astrophysical Journal* 270 (1983) 365.; M. Milgrom, *Scientific American* 287(2) (2002) 42.
- [8] D. Clower et al. *Astrophysical Journal* 648 (2006) 109.
- [9] G. Steigman and M.S. Turner, *Nucl. Phys.* B253, 375, 1985.
- [10] G. Jungman, M. Kamionkowski, and K. Griest, *Phys. Rep.* 267, (1996) 195;
- [11] S. Arrenberg et al., *Phys. Rev. D* 78 (2008) 056002.
- [12] L. Roszkowski, *Pramana J. Phys.* 62, (2004) 389 .
- [13] J.D. Lewin and P.F. Smith, *Astropart. Phys.* 6 (1996) 87.
- [14] Z. Ahmed et al., *Phys. Rev. Lett.* 102 (2009) 011301.
- [15] J. Angle et al., *Phys. Rev. Lett.* 100 (2008) 21303.
- [16] Y. Suzuki, arXiv:hep-ph/0008296.
- [17] E. Behnke et al., *Science* 319 (2008) 933.
- [18] H.S. Lee et al., *Phys. Rev. Lett.* 99 (2007) 091301.
- [19] J. Angle et al., *Phys. Rev. Lett.* 101 (2008) 091301.
- [20] R. Bernabei et al., *Riv. Nuovo Cim.* 26N1 (2003) 1.
- [21] R. Bernabei et al., *Eur. Phys. J. C* 56 (2008) 333.
- [22] A. Bottino et al., *Phys. Rev. D* 77 (2007) 015002.
- [23] A. Bottino et al., *Phys. Rev. D* 78 (2008) 083520.
- [24] J. L. Feng et al., *Phys. Lett. B* 670 (2008) 37.
- [25] S. Chang et al., *Phys. Rev. D* 79 (2008) 115011.
- [26] C. Savage et al., *JCAP* 0904 (2009) 010.
- [27] F. Aubin et al., *New J. Phys.* 10 (2008) 103017.
- [28] D. Tucker-Smith and N. Weiner, *Phys. Rev. D* 64 (2001) 043502.
- [29] S. Chang et al. *Phys. Rev. D* 79 (2009) 043513.
- [30] G. Angloher et al., *Astroparticle Physics* 31 (2009) 270.
- [31] V. N. Lebedenko et al., arXiv:0812.1150 [astro-ph].
- [32] J. Angle et al., arXiv:0910.3698.
- [33] Z. Ahmed et al., arXiv:0907.1438.
- [34] R. Ruiz de Austri, R. Trotta, L. Roszkowski, *JHEP* 0605 (2006) 002.